

# Size-Dependent Large Amplitude Vibration Analysis of Nanoshells Using the Gurtin-Murdoch Model

H. Rouhi, R. Ansari\* and M. Darvizeh

Department of Mechanical Engineering, University of Guilan, P.O. Box 3756, Rasht, Iran.

(\*) Corresponding author: r\_ansari@guilan.ac.ir  
(Received: 12 May 2016 and Accepted: 03 August 2016)

## Abstract

Shell-type nanostructures have recently attracted a lot of attention due to their several applications. The surface stress effect plays an important role in the mechanical behavior of such structures because of their large surface-to-volume ratio. In this paper, an analytical approach is presented for analyzing the geometrically nonlinear free vibrations of cylindrical nanoshells. In order to capture the surface stress influence, the Gurtin-Murdoch continuum model is applied. First, the equations governing the nonlinear vibrations of the shell considering the surface stress effect are derived using an energy-based method. In the next step, a perturbation technique is utilized to obtain the frequency-amplitude curves of nanoshells. Various numerical results are given to investigate the vibrational behavior of nanoshells with different geometrical and surface material properties. It is shown that the surface stress significantly affects the nonlinear free vibration behavior of the nanoshells when they are very thin. Also, it is revealed that the effect of geometrical nonlinearity is more prominent when the surface residual stress is negative.

**Keywords:** Gurtin-Murdoch elasticity theory, Nanoshell, Large amplitude vibration, Surface stress, Analytical approach.

## 1. INTRODUCTION

Research on nanostructures including nanobeams, nanoplates, nanowires and nanotubes has attracted a lot of interest from the researchers of different fields during the past two decades [1-4]. Among them, nanoshells have become the focus of scientific attention in recent years owing to their interesting applications. Nanoscale shells can be used as sensors [5, 6], MRI contrast agents [7, 8], nanoneedles for intracellular injections [9], clinical applications [10], nanoreactors [11] and nanoinjectors for ink-jet printers [12].

Studying the mechanical characteristics of nanostructures is the topic of many research works in the literature. Accurate predicting the mechanical response of nanostructures is of great importance in some applications such as in nano-electro-mechanical systems (NEMS). A literature review reveals that a large number of the

theoretical investigations performed in this field are based on the continuum models. The wide applicability of continuum models is mainly due to their computational efficiency when they are compared with their atomistic counterparts. It should be noted that the classical continuum models are not suitable for the analyses of nanostructures since they are scale-free. It has been generally accepted that the mechanical behaviors of micro- and nanostructures are size-dependent. Hence, some modified continuum models including intrinsic length scales have been developed so far.

The nonlocal model developed by Eringen [13, 14] is a modified continuum model which can capture the size-dependent behavior of nanostructures. In this model, it is considered that the stress at a point is a function of strains at all

points in the continuum. There are different uses of such model in the bending [15-17], buckling [18-22] and vibration [23-29] analyses of nanostructures. For example, Yan et al. [15] presented closed-form solutions for the bending of nanobeams and nanoplates based upon Eringen's nonlocal mode. Ansari and Rouhi [19] developed a nonlocal Flügge shell model for the buckling analysis of multi-walled carbon nanotubes under the action of thermal loads. Pradhan and Kumar [28] studied the vibrations of orthotropic graphene sheets embedded in Pasternak elastic medium within the framework of nonlocal elasticity theory. Gurses et al. [29] addressed the vibration problem of annular sector nanoplates based on the nonlocal elasticity theory by eight-node discrete singular convolution transformation. Also, it has been indicated that the accuracy of the results of Eringen's model is comparable to that of molecular dynamics (MD) simulations provided that the nonlocal parameter is suitably calibrated [30-35].

The Gurtin-Murdoch model [36, 37] is another size-dependent continuum model with wide applications in the problems of nanostructures. This model is originally developed for capturing the surface stress effect on the behavior of structures. The surface stress effect can be explained by the fact that atoms at or near a free surface of a solid body have different equilibrium requirements as compared to those within the bulk of material due to dissimilar environmental conditions. Because the energies of surface atoms are different from those of bulk atoms, creation of a surface leads to an excess free energy that is called as the surface free energy. The surface stress is also defined based on the variation of surface free energy with the surface strain [38]. Since nanostructures have high surface-to-volume ratios, the surface stress can significantly affect their mechanical behavior. Based on the Gurtin-Murdoch model, the surface stress is formulated as a function of the

deformation gradient, and the surface is modeled as a mathematical layer with zero thickness perfectly bonded to the bulk phase without slipping.

Up to now, many researchers have applied the Gurtin-Murdoch model to the problems of nanobeams [39-44], nanowires [45-47], nanoplates [48-53]. However, research into the mechanical behaviors of nanoshells using the Gurtin-Murdoch model is limited [54, 55]. Recently, Rouhi et al. [55] developed a size-dependent shell model based upon the Gurtin-Murdoch model to study the linear free vibrations of cylindrical nanoshells with the consideration of surface effects.

Understanding the vibration behavior of nanostructures is of great importance for many devices like oscillators, clocks and sensors; and in some applications, nanostructures show the large-amplitude vibration behavior. For example, because of various sources of nonlinearities such as mid-plane stretching effects, nonlinear behaviors including softening- or hardening-type frequency responses are observed in NEMS resonators. The effective design of such nonlinear systems necessitates analyzing their nonlinear dynamics properly. In this regard, analytical solution approaches are efficient tools to accomplish this aim.

Motivated by these considerations and considering the fact that the surface stress can significantly affect the behavior of nanoshells, the large amplitude vibrations of cylindrical nanoshells are investigated in the present article in the context of Gurtin-Murdoch surface elasticity theory by an analytical method. To this end, using the classical shell theory in conjunction with the Gurtin-Murdoch model, a size-dependent shell model is developed. The geometrical nonlinearity is incorporated into the shell formulation based on the von Kármán's hypothesis. The governing equations including the surface stress effect are obtained by Hamilton's principle which are then solved via the multiple scale method analytically. In the numerical

results section, the effects of geometrical parameters and surface properties on the nonlinear vibrations of nanoshell are studied. A comparison is also made between the predictions of Gurtin-Murdoch model and its classical counterpart.

## 2. PROBLEM FORMULATION

Figure 1 shows a circular cylindrical nanoshell with length  $L$ , thickness  $h$ , and mid-surface radius  $R$ . It is considered that the nanoshell has a bulk part and two additional thin surface layers (inner and outer layers). By selecting a coordinate system whose origin is located on the middle surface of the nanoshell, coordinates of a typical point in the axial, circumferential and radial directions are denoted by  $x$ ,  $y$  and  $z$ , respectively.

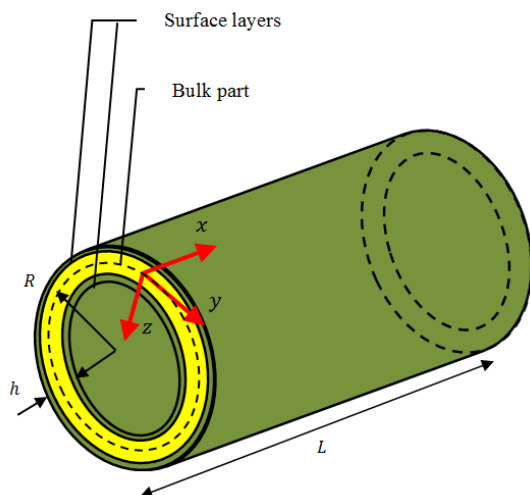


**Figure 1.** Schematic view of a circular cylindrical nanoshell with bulk and surface phases.

The displacement field can be expressed as [56]

$$\begin{aligned} u_x(t, x, y, z) &= u(t, x, y) - z \frac{\partial w(t, x, y)}{\partial x} \\ u_y(t, x, y, z) &= v(t, x, y) - z \frac{\partial w(t, x, y)}{\partial y} \\ u_z(t, x, y, z) &= w(t, x, y) \end{aligned} \quad (1)$$

where  $u$ ,  $v$  and  $w$  are the middle surface displacements. Also,  $t$  denotes time. Based

on von Kármán's hypothesis, the kinematic relations are given as [57]

$$\begin{aligned} \begin{Bmatrix} \varepsilon_{xx} \\ \varepsilon_{yy} \\ \gamma_{xy} \end{Bmatrix} &= \begin{Bmatrix} \varepsilon_{xx}^0 \\ \varepsilon_{yy}^0 \\ \gamma_{xy}^0 \end{Bmatrix} - z \begin{Bmatrix} \kappa_{xx} \\ \kappa_{yy} \\ \kappa_{xy} \end{Bmatrix} \\ &= \begin{Bmatrix} \frac{\partial u}{\partial x} + \frac{1}{2} \left( \frac{\partial w}{\partial x} \right)^2 \\ \frac{\partial v}{\partial y} + \frac{w}{R} + \frac{1}{2} \left( \frac{\partial w}{\partial y} \right)^2 \\ \frac{\partial u}{\partial y} + \frac{\partial v}{\partial x} + \frac{\partial w}{\partial x} \frac{\partial w}{\partial y} \end{Bmatrix} - z \begin{Bmatrix} \frac{\partial^2 w}{\partial x^2} \\ \frac{\partial^2 w}{\partial y^2} \\ 2 \frac{\partial^2 w}{\partial x \partial y} \end{Bmatrix} \end{aligned} \quad (2)$$

The constitutive relations of bulk part are formulated as

$$\begin{Bmatrix} \sigma_{xx} \\ \sigma_{yy} \\ \sigma_{xy} \\ \sigma_{xz} \\ \sigma_{yz} \end{Bmatrix} = \begin{bmatrix} \lambda + 2\mu & \lambda & 0 \\ \lambda & \lambda + 2\mu & 0 \\ 0 & 0 & \mu \\ 0 & 0 & 0 \\ 0 & 0 & 0 \end{bmatrix} \begin{Bmatrix} \varepsilon_{xx} \\ \varepsilon_{yy} \\ \gamma_{xy} \end{Bmatrix} \quad (3)$$

where  $\lambda = E\nu/(1-\nu^2)$ ,  $\mu = E/(2(1+\nu))$  are classical Lamé's parameters ( $E$  and  $\nu$  are Young's modulus and Poisson's ratio of bulk part, respectively).

Using the Gurtin-Murdoch model, the constitutive relations of bulk part are also formulated as [36]

$$\sigma_{\alpha\beta}^s = \tau^s \delta_{\alpha\beta} + (\tau^s + \lambda^s) \varepsilon_{\gamma\gamma} \delta_{\alpha\beta} + 2(\mu^s - \tau^s) \varepsilon_{\alpha\beta} + \tau^s \mu_{\alpha,\beta}^s \quad (4)$$

$$\sigma_{\alpha z}^s = \tau^s u_{z,\alpha}^s \quad (\alpha, \beta = x, y)$$

in which  $\lambda^s$  and  $\mu^s$  are surface Lamé's parameters.  $E^s$ ,  $\nu^s$  and  $\rho^s$  are respectively the surface elasticity modulus, Poisson's ratio and density of surface layers. Moreover,  $\tau^s$  stands for the surface residual stress.

Using Eqs. (2) and (4), the surface stress components in terms of the displacement components are obtained as

$$\begin{aligned} \sigma_{xx}^s &= (\lambda^s + 2\mu^s) \varepsilon_{xx} + (\tau^s + \lambda^s) \varepsilon_{yy} \\ &\quad - \frac{\tau^s}{2} \left( \frac{\partial w}{\partial x} \right)^2 + \tau^s \\ \sigma_{xz}^s &= \tau^s \frac{\partial w}{\partial x} \end{aligned}$$

$$\begin{aligned}
\sigma_{yy}^s &= (\lambda^s + 2\mu^s)\varepsilon_{yy} + (\tau^s + \lambda^s)\varepsilon_{xx} \\
&\quad - \tau^s \left( \frac{w}{R} + \frac{1}{2} \left( \frac{\partial w}{\partial y} \right)^2 \right) + \tau^s \\
\sigma_{yz}^s &= \tau^s \frac{\partial w}{\partial y} \\
\sigma_{xy}^s &= \mu^s \gamma_{xy} - \tau^s \left( \frac{\partial v}{\partial x} + \frac{\partial w}{\partial x} \frac{\partial w}{\partial y} - z \frac{\partial^2 w}{\partial x \partial y} \right) \\
\sigma_{yx}^s &= \mu^s \gamma_{xy} - \tau^s \left( \frac{\partial u}{\partial y} + \frac{\partial w}{\partial x} \frac{\partial w}{\partial y} - z \frac{\partial^2 w}{\partial x \partial y} \right)
\end{aligned} \tag{5}$$

In the classic continuum models, it is assumed that  $\sigma_{zz} = 0$ . This is because the stress component  $\sigma_{zz}$  is small in comparison with other normal stresses. But, this assumption does not satisfy the surface conditions of the Gurtin-Murdoch continuum model. To tackle this problem, it is supposed that the stress component  $\sigma_{zz}$  varies linearly through the thickness and satisfies the balance conditions on the surfaces [58]. According to this assumption,  $\sigma_{zz}$  can be obtained as

$$\begin{aligned}
\sigma_{zz} &= \frac{\left( \frac{\partial \sigma_{xz}^+}{\partial x} + \frac{\partial \sigma_{yz}^+}{\partial y} - \rho^{s+} \frac{\partial^2 w}{\partial t^2} \right) - \left( \frac{\partial \sigma_{xz}^-}{\partial x} + \frac{\partial \sigma_{yz}^-}{\partial y} - \rho^{s-} \frac{\partial^2 w}{\partial t^2} \right)}{2} \\
&\quad + \frac{\left( \frac{\partial \sigma_{xz}^+}{\partial x} + \frac{\partial \sigma_{yz}^+}{\partial y} - \rho^{s+} \frac{\partial^2 w}{\partial t^2} \right) + \left( \frac{\partial \sigma_{xz}^-}{\partial x} + \frac{\partial \sigma_{yz}^-}{\partial y} - \rho^{s-} \frac{\partial^2 w}{\partial t^2} \right)}{h} z
\end{aligned} \tag{6}$$

Using Eq. (5),  $\sigma_{zz}$  can be written as follows

$$\sigma_{zz} = \frac{2z}{h} \left( \tau^s \frac{\partial^2 w}{\partial x^2} + \tau^s \frac{\partial^2 w}{\partial y^2} - \rho^s \frac{\partial^2 w}{\partial t^2} \right) \tag{7}$$

Now, the relations of normal stresses  $(\sigma_{xx}, \sigma_{yy})$  for the bulk of the nanoshell are formulated as

$$\begin{aligned}
\sigma_{xx} &= (\lambda + 2\mu)\varepsilon_{xx} + \lambda\varepsilon_{yy} + \frac{\nu\sigma_{zz}}{(1-\nu)} \\
\sigma_{yy} &= (\lambda + 2\mu)\varepsilon_{yy} + \lambda\varepsilon_{xx} + \frac{\nu\sigma_{zz}}{(1-\nu)}
\end{aligned} \tag{8}$$

The total strain energy is given by

$$\begin{aligned}
\Pi_s &= \frac{1}{2} \int_S \int_{-\frac{h}{2}}^{\frac{h}{2}} \sigma_{ij} \varepsilon_{ij} dz dS \\
&\quad + \frac{1}{2} \left( \int_{S^+} \sigma_{ij}^s \varepsilon_{ij} dS^+ + \int_{S^-} \sigma_{ij}^s \varepsilon_{ij} dS^- \right)
\end{aligned}$$

$$\begin{aligned}
&= \frac{1}{2} \int_S \left\{ \bar{N}_{xx} \varepsilon_{xx}^0 + \bar{N}_{yy} \varepsilon_{yy}^0 + \bar{N}_{xy} \gamma_{xy}^0 - \bar{M}_{xx} \kappa_{xx} \right. \\
&\quad \left. - \bar{M}_{yy} \kappa_{yy} - 2\bar{M}_{xy} \kappa_{xy} + Q_x^s \frac{\partial w}{\partial x} \right. \\
&\quad \left. + Q_y^s \frac{\partial w}{\partial y} \right\} dS
\end{aligned} \tag{9}$$

in which  $S$  denotes the area occupied by the middle plane of the nanoshell. The in-plane force resultants, bending moments and shear forces are written as

$$\begin{aligned}
\bar{N}_{xx} &= N_{xx} + \sigma_{xx}^{s+} + \sigma_{xx}^{s-} \\
&= A_{11}^* \varepsilon_{xx}^0 + A_{12}^* \varepsilon_{yy}^0 - \tau^s \left( \frac{\partial w}{\partial x} \right)^2 + 2\tau^s \\
\bar{N}_{yy} &= N_{yy} + \sigma_{yy}^{s+} + \sigma_{yy}^{s-} \\
&= A_{11}^* \varepsilon_{yy}^0 + A_{12}^* \varepsilon_{xx}^0 - \tau^s \left( \frac{2w}{R} + \left( \frac{\partial w}{\partial y} \right)^2 \right) + 2\tau^s \\
\bar{N}_{xy} &= N_{xy} + \frac{1}{2} (\sigma_{xy}^{s+} + \sigma_{yx}^{s+} + \sigma_{xy}^{s-} + \sigma_{yx}^{s-}) \\
&= A_{55}^* \gamma_{xy}^0 \\
\bar{M}_{xx} &= M_{xx} + \frac{h}{2} (\sigma_{xx}^{s+} - \sigma_{xx}^{s-}) \\
&= -D_{11}^* \kappa_{xx} - D_{12}^* \kappa_{yy} \\
&\quad + E_{11}^* \left( \frac{\partial^2 w}{\partial x^2} + \frac{\partial^2 w}{\partial y^2} \right) - G_{11}^* \frac{\partial^2 w}{\partial t^2} \\
\bar{M}_{yy} &= M_{yy} + \frac{h}{2} (\sigma_{yy}^{s+} - \sigma_{yy}^{s-}) \\
&= -D_{11}^* \kappa_{yy} - D_{12}^* \kappa_{xx} + E_{11}^* \left( \frac{\partial^2 w}{\partial x^2} + \frac{\partial^2 w}{\partial y^2} \right) \\
&\quad - G_{11}^* \frac{\partial^2 w}{\partial t^2} \\
\bar{M}_{xy} &= M_{xy} + \frac{h}{4} (\sigma_{xy}^{s+} + \sigma_{yx}^{s+} - \sigma_{xy}^{s-} - \sigma_{yx}^{s-}) \\
&= -D_{55}^* \kappa_{xy} \\
Q_x^s &= \sigma_{xz}^{s-} + \sigma_{xz}^{s+} = 2\tau^s \frac{\partial w}{\partial x} \\
Q_y^s &= \sigma_{yz}^{s-} + \sigma_{yz}^{s+} = 2\tau^s \frac{\partial w}{\partial y}
\end{aligned} \tag{10}$$

in which

$$\begin{aligned}
\left\{ \begin{matrix} N_{xx} \\ N_{yy} \\ N_{xy} \end{matrix} \right\} &= \int_{-\frac{h}{2}}^{\frac{h}{2}} \left\{ \begin{matrix} \sigma_{xx} \\ \sigma_{yy} \\ \sigma_{xy} \end{matrix} \right\} dz \\
\left\{ \begin{matrix} M_{xx} \\ M_{yy} \\ M_{xy} \end{matrix} \right\} &= \int_{-\frac{h}{2}}^{\frac{h}{2}} \left\{ \begin{matrix} \sigma_{xx} \\ \sigma_{yy} \\ \sigma_{xy} \end{matrix} \right\} z dz
\end{aligned} \tag{11a}$$

$$\begin{aligned}
A_{11}^* &= (\lambda + 2\mu)h + 2(\lambda^s + 2\mu^s) \\
A_{12}^* &= \lambda h + 2\tau^s + 2\lambda^s \\
A_{55}^* &= \mu h + 2\mu^s - \tau^s \\
A_{55} &= \mu h
\end{aligned}$$

$$\begin{aligned}
D_{11}^* &= \frac{(\lambda + 2\mu)h^3}{12} + \frac{(\lambda^s + 2\mu^s)h^2}{2} \\
D_{12}^* &= \frac{\lambda h^3}{12} + \frac{(\tau^s + \lambda^s)h^2}{2} \\
E_{11}^* &= \frac{\nu h^2 \tau^s}{6(1-\nu)} \\
D_{55}^* &= \frac{\mu h^3}{12} + \frac{(2\mu^s - \tau^s)h^2}{4} \\
G_{11}^* &= \frac{\rho^s \nu h^2}{6(1-\nu)}
\end{aligned} \tag{11b}$$

The kinetic energy is

$$\Pi_T = \frac{1}{2} \int_S \left\{ I_0^* \left[ \left( \frac{\partial u}{\partial t} \right)^2 + \left( \frac{\partial v}{\partial t} \right)^2 + \left( \frac{\partial w}{\partial t} \right)^2 \right] \right\} dS \tag{12}$$

where  $I_0^* = \rho h + 2\rho^s$ .

Hamilton's principle states that

$$\delta \int_{t_1}^{t_2} (\Pi_T - \Pi_S) dt = 0 \tag{13}$$

By taking the variations of  $u$ ,  $v$  and  $w$ , integrating by parts, and by putting coefficients of  $\delta u$ ,  $\delta v$  and  $\delta w$  equal to zero, the size-dependent governing equations of the nanoshell including the surface stress effect are derived as

$$\begin{aligned}
\frac{\partial \bar{N}_{xx}}{\partial x} + \frac{\partial \bar{N}_{xy}}{\partial y} &= I_0^* \frac{\partial^2 u}{\partial t^2} \\
\frac{\partial \bar{N}_{xy}}{\partial x} + \frac{\partial \bar{N}_{yy}}{\partial y} &= I_0^* \frac{\partial^2 v}{\partial t^2} \\
\frac{\partial^2 \bar{M}_{xx}}{\partial x^2} + 2 \frac{\partial^2 \bar{M}_{xy}}{\partial y \partial x} + \frac{\partial^2 \bar{M}_{yy}}{\partial y^2} - \frac{\bar{N}_{yy}}{R} \\
+ \frac{\partial Q_x^s}{\partial x} + \frac{\partial Q_y^s}{\partial y} + \frac{\partial}{\partial x} \left( \bar{N}_{xx} \frac{\partial w}{\partial x} \right) \\
+ \frac{\partial}{\partial y} \left( \bar{N}_{yy} \frac{\partial w}{\partial y} \right) + \frac{\partial}{\partial x} \left( \bar{N}_{xy} \frac{\partial w}{\partial y} \right) \\
+ \frac{\partial}{\partial y} \left( \bar{N}_{xy} \frac{\partial w}{\partial x} \right) &= I_0^* \frac{\partial^2 w}{\partial t^2}
\end{aligned} \tag{14}$$

The corresponding boundary conditions are also derived as

$$\begin{aligned}
\delta u &= 0 \text{ or } (\bar{N}_{xx})n_x + (\bar{N}_{xy})n_y = 0 \\
\delta v &= 0 \text{ or } (\bar{N}_{yx})n_x + (\bar{N}_{yy})n_y = 0 \\
\delta w &= 0 \text{ or } \\
\left( Q_x^s + \frac{\partial \bar{M}_{xx}}{\partial x} + \frac{\partial \bar{M}_{xy}}{\partial y} + \bar{N}_{xx} \frac{\partial w}{\partial x} + \bar{N}_{xy} \frac{\partial w}{\partial y} \right) n_x \\
+ \left( Q_y^s + \frac{\partial \bar{M}_{xy}}{\partial x} + \frac{\partial \bar{M}_{yy}}{\partial y} + \bar{N}_{yy} \frac{\partial w}{\partial y} + \bar{N}_{xy} \frac{\partial w}{\partial x} \right) n_y
\end{aligned} \tag{15}$$

$$\begin{aligned}
&= 0 \\
\delta \left( \frac{\partial w}{\partial x} \right) &= 0 \text{ or } (\bar{M}_{xx})n_x + (\bar{M}_{xy})n_y = 0 \\
\delta \left( \frac{\partial w}{\partial y} \right) &= 0 \text{ or } (\bar{M}_{xy})n_x + (\bar{M}_{yy})n_y = 0
\end{aligned}$$

By introducing Eqs. (10) into (14), the governing equations are rewritten in terms of displacement components as follows

$$\begin{aligned}
A_{11}^* \left( \frac{\partial^2 u}{\partial x^2} + \frac{\partial w}{\partial x} \frac{\partial^2 w}{\partial x^2} \right) \\
+ (A_{12}^* + A_{55}^*) \left( \frac{\partial v}{\partial x \partial y} + \frac{\partial w}{\partial y} \frac{\partial w}{\partial x \partial y} \right) \\
+ \frac{A_{12}^*}{R} \frac{\partial w}{\partial x} + A_{55}^* \left( \frac{\partial^2 u}{\partial y^2} + \frac{\partial w}{\partial x} \frac{\partial^2 w}{\partial y^2} \right) \\
- 2\tau^s \frac{\partial w}{\partial x} \frac{\partial^2 w}{\partial x^2} = I_0^* \frac{\partial^2 u}{\partial t^2} \\
A_{11}^* \left( \frac{\partial^2 v}{\partial y^2} + \frac{1}{R} \frac{\partial w}{\partial y} + \frac{\partial w}{\partial y} \frac{\partial^2 w}{\partial y^2} \right) \\
+ (A_{12}^* + A_{55}^*) \left( \frac{\partial u}{\partial x \partial y} + \frac{\partial w}{\partial x} \frac{\partial w}{\partial x \partial y} \right) \\
+ A_{55}^* \left( \frac{\partial^2 v}{\partial x^2} + \frac{\partial w}{\partial y} \frac{\partial^2 w}{\partial x^2} \right) \\
- 2\tau^s \left( \frac{\partial w}{\partial y} \frac{\partial^2 w}{\partial y^2} + \frac{1}{R} \frac{\partial w}{\partial y} \right) = I_0^* \frac{\partial^2 v}{\partial t^2} \\
-D_{11}^* \left( \frac{\partial^4 w}{\partial x^4} + \frac{\partial^4 w}{\partial y^4} \right) \\
+ E_{11}^* \left( \frac{\partial^4 w}{\partial x^4} + 2 \frac{\partial^4 w}{\partial x^2 \partial y^2} + \frac{\partial^4 w}{\partial y^4} \right) \\
- 2(2D_{55}^* + D_{12}^*) \frac{\partial^4 w}{\partial x^2 \partial y^2} \\
- G_{11}^* \left( \frac{\partial^4 w}{\partial t^2 \partial x^2} + \frac{\partial^4 w}{\partial t^2 \partial y^2} \right) \\
+ 2\tau^s \left( \frac{\partial^2 w}{\partial x^2} + \frac{\partial^2 w}{\partial y^2} \right) \\
- \frac{1}{R} \left( A_{11}^* \left( \frac{\partial v}{\partial y} + \frac{w}{R} + \frac{1}{2} \left( \frac{\partial w}{\partial y} \right)^2 \right) \right. \\
+ A_{12}^* \left( \frac{\partial u}{\partial x} + \frac{1}{2} \left( \frac{\partial w}{\partial x} \right)^2 \right) \\
- \tau^s \left( \frac{2w}{R} + \left( \frac{\partial w}{\partial y} \right)^2 \right) + 2\tau^s \left. \right) \\
+ \frac{\partial}{\partial x} \left( \bar{N}_{xx} \frac{\partial w}{\partial x} \right) + \frac{\partial}{\partial y} \left( \bar{N}_{yy} \frac{\partial w}{\partial y} \right) \\
+ \frac{\partial}{\partial x} \left( \bar{N}_{xy} \frac{\partial w}{\partial y} \right) + \frac{\partial}{\partial y} \left( \bar{N}_{xy} \frac{\partial w}{\partial x} \right) \\
= I_0^* \frac{\partial^2 w}{\partial t^2}
\end{aligned} \tag{16}$$

### 3. ANALYTICAL SOLUTION

The simply-supported boundary conditions are given by

$$v = w = M_{xx} = N_{xx} = 0 \text{ at } x = 0, L \quad (17)$$

The displacement components can be approximated as

$$\begin{cases} u(x, y, t) \\ v(x, y, t) \\ w(x, y, t) \end{cases} = \sum_{n=1}^{\infty} \sum_{m=1}^{\infty} \begin{cases} u_{mn}(t)U_{mn}(x, y) \\ v_{mn}(t)V_{mn}(x, y) \\ w_{mn}(t)W_{mn}(x, y) \end{cases} \quad (18)$$

$U_{mn}(x, y), V_{mn}(x, y), W_{mn}(x, y)$  should be properly selected such that exactly satisfy boundary conditions of Eq. (17). To this end, one can write

$$\begin{cases} u(x, y, t) \\ v(x, y, t) \\ w(x, y, t) \end{cases} \quad (19) \\ = \sum_{n=1}^{\infty} \sum_{m=1}^{\infty} \begin{cases} u_{mn}(t) \cos(\lambda_m x) \sin(\lambda_n y) \\ v_{mn}(t) \sin(\lambda_m x) \cos(\lambda_n y) \\ w_{mn}(t) \sin(\lambda_m x) \cos(\lambda_n y) \end{cases}$$

in which

$$\lambda_m = m\pi/L, \lambda_n = n/R \quad (20)$$

Eq. (19) is substituted into (16), and then the Galerkin method is used to arrive at

$$\begin{aligned} C_{11}u_{mn}(t) + C_{12}v_{mn}(t) + C_{13}w_{mn}(t) &= \ddot{u}_{mn}(t) \\ C_{21}u_{mn}(t) + C_{22}v_{mn}(t) + C_{23}w_{mn}(t) &= \ddot{v}_{mn}(t) \\ C_{31}u_{mn}(t) + C_{32}v_{mn}(t) + C_{33}w_{mn}(t) \\ + C_{34}w_{mn}^3(t) &= \ddot{w}_{mn}(t) \end{aligned} \quad (21)$$

where

$$\begin{aligned} C_{11} &= -\Gamma^{-1} \left( \frac{A_{55}^* L n^2 \pi}{2R} + \frac{A_{11}^* m^2 \pi^3 R}{2L} \right) \\ C_{12} &= -\Gamma^{-1} \left( \frac{A_{12}^* + A_{55}^*}{2} \right) m n \pi^2 \\ C_{13} &= \Gamma^{-1} \frac{m \pi^2 A_{12}^*}{2} \\ C_{21} &= -\Gamma^{-1} \left( \frac{A_{12}^* + A_{55}^*}{2} \right) m n \pi^2 \\ C_{22} &= -\Gamma^{-1} \left( \frac{A_{11}^* L n^2 \pi}{2R} + \frac{A_{55}^* m^2 \pi^3 R}{2L} \right) \\ C_{23} &= \Gamma^{-1} \frac{L n \pi (A_{11}^* - 2\tau^5)}{2R} \\ C_{31} &= (\Lambda + \Gamma)^{-1} \frac{m \pi^2 A_{12}^*}{2} \\ C_{32} &= (\Lambda + \Gamma)^{-1} \frac{L n \pi A_{11}^*}{2R} \end{aligned}$$

$$\begin{aligned} C_{33} &= \frac{\pi}{2L^3 R^3} (\Lambda + \Gamma)^{-1} (-2(D_{12}^* + 2D_{55}^* \\ &\quad - E_{11}^*)L^2 m^2 n^2 \pi^2 R^2 - (D_{11}^* \\ &\quad - E_{11}^*)(L^4 n^4 + m^4 \pi^4 R^4) \\ &\quad - 4L^2 R^2 (L^2 n^2 + m^2 \pi^2 R^2) \tau^5 \\ &\quad - L^4 R^2 (A_{11}^* - 2\tau^5)) \\ C_{34} &= ((-4(A_{12}^* + A_{55}^*)L^2 m^2 n^2 \pi^3 R^2 \\ &\quad - 9A_{11}^* (L^4 n^4 \pi + m^4 \pi^5 R^4) \\ &\quad + 18\pi (L^4 n^4 + m^4 \pi^4 R^4) \tau^5) / (64L^3 R^3)) \times \\ &\quad (\Lambda + \Gamma)^{-1} \\ \Gamma &= I_0^* \frac{\pi L R}{2}, \Lambda = -\frac{G_{11}^* \pi (L^2 n^2 + m^2 \pi^2 R^2)}{2LR} \end{aligned} \quad (22)$$

The effect of transverse inertia term is dominant. Hence, all the inertia terms related to  $U_{mn}$  and  $V_{mn}$  in Eqs. (21a) and (21b) can be neglected with an adequate accuracy. After such approximation, the resulting equations with respect to  $U_{mn}$  and  $V_{mn}$  are solved and then the results are inserted into Eq. (21c). Accordingly, the following governing differential equation of transverse motion is achieved

$$\ddot{W}_{mn}(t) + P_1 W_{mn}(t) + P_2 W_{mn}^3(t) = 0 \quad (23)$$

where

$$\begin{aligned} P_1 &= (C_{13}C_{22}C_{31} - C_{12}C_{23}C_{31} - C_{13}C_{21}C_{32} \\ &\quad + C_{11}C_{23}C_{32}) / (C_{11}C_{22} - C_{12}C_{21}) - C_{33} \\ P_2 &= -C_{34} \end{aligned} \quad (24)$$

Note that

$$\omega_{mnl} = \sqrt{P_1} \quad (25)$$

By considering the linear parts of Eq. (21), the natural frequencies of the nanoshell are computed by solving the following determinant

$$\begin{vmatrix} l_{11} + \omega_{0mnl} & l_{12} & l_{13} \\ l_{21} & l_{22} + \omega_{0mnl} & l_{23} \\ l_{31} & l_{32} & l_{33} + \omega_{0mnl} \end{vmatrix} = 0 \quad (26)$$

Three frequencies in the axial, circumferential and radial directions are obtained by solving this equation. The smallest frequency is considered. The initial conditions is

$$w|_{t=0} = w_{max}, \quad \frac{\partial w}{\partial t}|_{t=0} = 0 \quad (27)$$

The multiple scales method is employed in order to solve Eq. (23) [59]. To this end, the following dimensionless parameters are defined first

$$W = \theta \bar{w}, \quad t = \omega \bar{t} \quad (28)$$

Thus, one can write

$$\frac{d^2 \bar{w}}{d\bar{t}^2} + P_2 \omega^2 \theta^2 w^3_{mn} + P_1 \omega^2 \bar{w} = 0 \quad (29)$$

$$\bar{w}|_{\bar{t}=0} = \frac{w_{max}}{\theta}, \quad \frac{\partial \bar{w}}{\partial \bar{t}}|_{\bar{t}=0} = 0$$

So as to set the dimensionless initial condition and the dimensionless main natural frequency equal to unity, the following relations are given

$$\theta = w_{max}, \quad \omega = \sqrt{\frac{1}{P_1}} \quad (30)$$

Therefore

$$\frac{d^2 \bar{w}}{d\bar{t}^2} + \beta_2 w^3_{mn} + \bar{w} = 0 \quad (31)$$

$$\bar{w}|_{\bar{t}=0} = 1, \quad \frac{\partial \bar{w}}{\partial \bar{t}}|_{\bar{t}=0} = 0$$

where  $\beta_2 = \frac{P_2}{P_1} w^2_{max}$ . The scaled times  $T_n$  are defined as

$$T_n = \varepsilon^n t, \quad n = 1, 2, 3, \dots \quad (32)$$

The chain rule is used as

$$\frac{d}{dt} = D_0 + \varepsilon D_1 + \dots \quad (33)$$

$$\frac{d^2}{dt^2} = D_0^2 + 2\varepsilon D_0 D_1 + \varepsilon^2 (D_1^2 + 2D_0 D_2) + \dots$$

in which

$$D_n = \frac{\partial}{\partial T_n}, \quad n = 1, 2, 3, \dots \quad (34)$$

Using the perturbation technique, the response  $\bar{w}$  can be expanded with respect to  $\varepsilon$  as

$$\bar{w}(\bar{t}; \varepsilon) = \varepsilon \bar{w}_1(T_0, T_1, T_2, \dots) + \varepsilon^2 \bar{w}_2(T_0, T_1, T_2, \dots) + \varepsilon^3 \bar{w}_3(T_0, T_1, T_2, \dots) \quad (35)$$

Substitution of Eqs. (33) and (35) into (31a) and equating the coefficients of same powers of  $\varepsilon$  to zero result in

$$\bar{w}_1 + D_0^2 \bar{w}_1 = 0 \quad (36a)$$

$$\bar{w}_2 + D_0^2 \bar{w}_2 = -2D_0 D_1 \bar{w}_1 \quad (36b)$$

$$\bar{w}_3 + D_0^2 \bar{w}_3 = -2D_0 D_1 \bar{w}_2 - D_1^2 \bar{w}_1 - 2D_0 D_2 \bar{w}_1 - \beta_2 \bar{w}_1^3 \quad (36c)$$

The solution of Eq. (36a) is

$$\bar{w}_1(T_0, T_1) = A(T_1) \exp(iT_0) + cc \quad (37)$$

Then

$$\bar{w}_2 + D_0^2 \bar{w}_2 = -2i \frac{\partial A}{\partial T_1} \exp(iT_0) + cc \quad (38)$$

By eliminating the terms that produce secular terms in  $\bar{w}_2$ ,

$$\frac{\partial A}{\partial T_1} = 0 \rightarrow \bar{w}_2 = 0 \quad (39)$$

Eq. (36c) is rewritten as

$$\bar{w}_3 + D_0^2 \bar{w}_3 = -(2iD_2 A + \beta_2 A^2 \bar{A}) \times \exp(iT_0) - \beta_2 A^3 \exp(3iT_0) + cc \quad (40)$$

Equating the secular term to zero leads to

$$2iD_2 A + \beta_2 A^2 \bar{A} = 0 \quad (41)$$

Eq. (41) is a complex differential equation. For its solution,  $A(T_2)$  can be expressed in polar form as

$$A(T_2) = \frac{1}{2} a(T_2) e^{i\phi(T_2)} \quad (42)$$

where  $a$  and  $\phi$  are real functions of  $T_2$ . By substituting Eq. (42) into (41) and separating the real and imaginary parts, the following differential equations governing  $a$  and  $\phi$  are obtained

$$\frac{da}{dT_2} = 0 \quad (43a)$$

$$a \frac{d\phi}{dT_2} = \frac{3\beta_2 a^3}{8} \quad (43b)$$

From Eq. (43b) one has

$$\phi = \frac{3\beta_2 a^2}{8} T_2 + \phi_0 \quad (44)$$

Now, Eq. (42) can be written as

$$A(T_2) = \frac{1}{2} a \exp\left(\frac{3\beta_2 a^2}{8} i \varepsilon^2 t + i \phi_0\right) \quad (45)$$

Substituting Eq. (45) into (40) leads to

$$\bar{w} = \varepsilon a \cos(\omega t + \phi_0) + O(\varepsilon^3) \quad (46)$$

The frequency of the system is obtained as

$$\omega = 1 + \frac{3\beta_2 a^2}{8} \varepsilon^2 \quad (47)$$

By applying the initial conditions from Eq. (31b) one has

$$\phi_0 = 0, a\varepsilon = 1 \quad (48)$$

As a result

$$\omega = 1 + \frac{3}{8} \beta_2 \quad (49)$$

#### 4. RESULTS AND DISCUSSION

To generate numerical results, the following material properties are considered for the bulk and surface parts [60, 61]:

$$E = 210 \text{ GPa}, \nu = 0.24, \rho = 2331 \text{ kg/m}^3$$

$$\mu^s = -2.774 \text{ N/m}, \lambda^s = -4.488 \text{ N/m}$$

$$\tau^s = 0.6048 \text{ N/m}, \rho^s = 3.17 \times 10^{-7} \text{ kg/m}^2$$

First, in Table 1, a comparison is made between the results obtained from the present shell model and those reported in [62] based on a Timoshenko beam model. This table shows the dimensionless frequencies for various length-to-radius ratios. It is observed that there is a good agreement between two sets of results.

In the following figures, the frequency ratio of the nanoshell is plotted versus its dimensionless vibration amplitude. These parameters are defined as

$$\text{Frequency ratio} = \omega_{NL}/\omega_L \quad (50a)$$

$$\text{Dimensionless amplitude} = w_{max}/h \quad (50b)$$

**Table 1.** Comparison between the present results and those of [62] ( $h = 1 \text{ nm}, d/h = 5$ ).

$L/R$	Present	[62]
45	0.2362	0.2341
90	0.2206	0.2204
135	0.2137	0.2126
200	0.2080	0.2076

where  $\omega_{NL}$  and  $\omega_L$  are the nonlinear and linear frequencies, respectively. Also,  $w_{max}$  denotes the maximum amplitude of vibration.

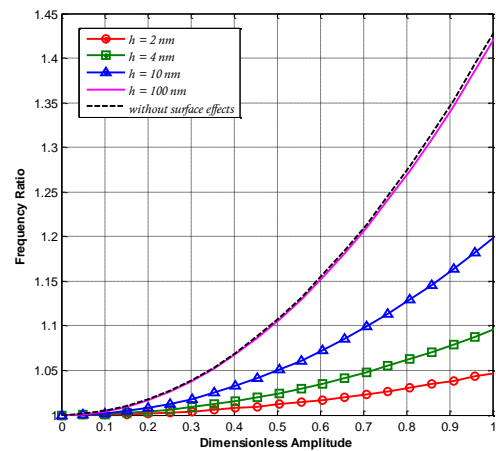


**Figure 2.** Comparison between the results of the Gurtin-Murdoch model and those of its classical counterpart ( $L = 0.5R, R = 100h$ ).

Figure 2 provides a comparison between the predictions of the Gurtin-Murdoch model and the prediction of the classical elasticity theory about the nonlinear free vibration behavior of the nanoshell. As shown, the Gurtin-Murdoch model is size-dependent, and different curves are obtained for various values of thickness. It is seen that there is a large difference between the results of two models as the nanoshell becomes very thin. This difference has its maximum value when the dimensionless amplitude is equal to unity. Figure 2 depicts that at a given dimensionless amplitude, the frequency ratio decreases as thickness of nanoshell decreases. It is also observed that the difference between the classical and non-classical results almost disappears as the

nanoshell becomes sufficiently thick. It means that the surface stress has an important influence on the nonlinear free vibration behavior of nanoshell with small thicknesses, but this influence can be neglected when the surface energy is negligible as compared to the energy of bulk of material. Moreover, the effect of geometrical nonlinearity can be seen in Fig. 2. The results show that the influence of geometrical nonlinearity becomes more prominent as the dimensionless amplitude increases. It is also seen that the nonlinear effect is weakened when the surface effects are taken into account.

**Table 2.** Comparison between the linear and nonlinear frequencies (GHz) of the nanoshell with considering surface effects for different values of thickness ( $R/h = 100$ ,  $L/R = 1$ ,  $w_{max} = h/2$ ).

$h(\text{nm})$	Nonlinear	Linear	Percentage difference
1	8.8601	8.8360	0.27
5	1.2387	1.2088	2.47
10	0.5277	0.5095	3.57
50	0.0892	0.0809	10.26
100	0.0429	0.0385	11.43

Furthermore, Table 2 provides a comparison between the nonlinear and linear frequencies of the nanoshell obtained based on the surface elasticity theory. This table indicates that the frequency of nanoshell increases when the geometrical nonlinearity is taken into account. However, the difference between the predictions of linear and nonlinear models can be neglected at small values of thickness for which the surface energies are dominant.

In Figure 3, the effect of surface residual stress on the nonlinear free vibration response of the nanoshell can be studied. Three values (positive, negative and zero) are considered for this parameter.

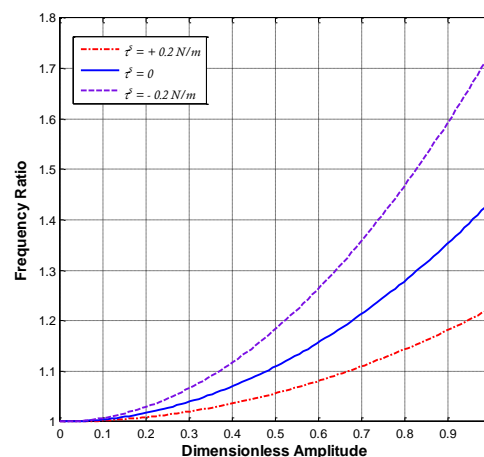


**Figure 3.** Nonlinear free vibration behavior of the nanoshell for different values of surface residual stress ( $L = 0.5R$ ,  $R = 100h$ ,  $h = 5\text{nm}$ ).

The figure clearly shows that the vibration behavior of the nanoshell is dependent on the sign of surface residual stress. One can see that at a given dimensionless amplitude, the frequency ratio associated with  $\tau^s = -0.2\text{ N/m}$  is greater than that associated with  $\tau^s = +0.2\text{ N/m}$ . It can be explained by the fact that the negative values of surface residual stress decreases the linear stiffness of the nanoshell, whereas the positive values have an increasing effect.

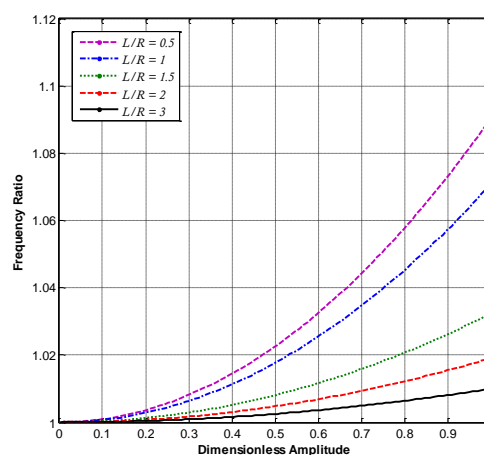


**Figure 4.** Nonlinear free vibration behavior of the nanoshell for different values of length-to-radius ratio ( $R = 200h$ ,  $h = 10\text{ nm}$ ).

Figure 4 indicates the nonlinear free vibration behavior of the nanoshell for different length-to-radius ratios ranging from 0.5 to 3. It is observed that the hardening-type behavior of the nanoshell is weakened as the length-to-radius ratio increases. This can be explained by the role of surface energies which are more prominent at large length-to-radius ratios. It should be noted that at a constant value of thickness, the surface energies increase with the increase of length-to-thickness ratio.

## 5. CONCLUSION

The Gurtin-Murdoch model was utilized in this paper in order to investigate the nonlinear free vibration characteristics of cylindrical nanoshells with the consideration of surface stress effect. The governing equations were derived using the classical shell theory together with Hamilton's principle. The Galerkin and multiple scales methods were also used to analytically solve the nonlinear free

vibration problem. Selected numerical results were presented to study the surface effects on the behavior of the nanoshell. It was concluded that the surface stress significantly affects the vibrational behavior of the nanoshell when it is very thin. The results showed that, due to the surface stress effect, the nonlinear hardening-type response of the nanoshell is weakened as the thickness decreases. It was also observed that the difference between the predictions of the Gurtin-Murdoch model and its classical counterpart can be neglected for sufficiently thick nanoshells. Another finding was that the nanoshell has different responses for positive and negative values of surface residual stress. It was shown that the effect of nonlinearity is more prominent when the surface residual stress is negative. The reason is that the compressive in-plane forces are generated in the nanoshell when surface residual stresses is negative.

## REFERENCES

1. Farhadian, N., Shariaty-Niassar, M., (2009). "Molecular Dynamics Simulation of Water in Single Wall Carbon Nanotube", *Int. J. Nanosci. Nanotechnol.*, 5: 53-62.
2. Basir Jafari, S., Malekfar, R., Khadem, S. E., (2011). "Radial Breathing Mode Frequency of Multi-Walled Carbon Nanotube Via Multiple-Elastic Thin Shell Theory", *Int. J. Nanosci. Nanotechnol.*, 7: 137-142.
3. Salehipour, H., Nahvi, H., Shahidi, A. R., (2016). "Exact analytical solution for free vibration of functionally graded micro/nanoplates via three-dimensional nonlocal elasticity", *Physica E*, 66: 350-358.
4. Wang, K. F., Wang, B. L., Kitamura, T., (2016). "A review on the application of modified continuum models in modeling and simulation of nanostructures" *Acta Mech. Sin.*, 32: 83-100.
5. Zhu, J., Li, J. -J., Zhao, J. -W., (2013). "Obtain Quadruple Intense Plasmonic Resonances from Multilayered Gold Nanoshells by Silver Coating: Application in Multiplex Sensing", *Plasmonics*, 8: 1493.
6. Kumar, C. S. S. R., (2007). "*Nanomaterials for Biosensors*", Wiley-VCH, Wein-heim.
7. Zabow, G., Dodd, S. J., Moreland, J., Koretsky, A. P., (2009). "The Fabrication of Uniform Cylindrical Nanoshells and Their Use as Spectrally Tunable MRI Contrast Agents", *Nanotechnology*, 20: 385301.
8. Zabow, G., Dodd, S., Moreland, J., Koretsky, A., (2010). "Multispectral MRI Contrast Through Cylindrical Nanoshell Agents", *Proc. Intl. Soc. Mag. Reson. Med.*, 18: 38.
9. Prinz, A. V., Prinz, V. Ya., Seleznev, V. A., "Microneedle in the Integral Version and Methods for its Fabrication," Parent of the Russian Federation, No. 2179458 RF, 7 A 61 M 5/32, Publ. 02.20.2002.
10. Khosroshahi, M. E., and Ghazanfari, L., 2011, "Synthesis of Three-Layered Magnetic Based Nanostructure for Clinical Application," *Int. J. Nanosci. Nanotechnol.*, 7: 57-64.
11. Deneke, C., Jin-Phillipp, N. Y., Loa, I., Schmidt, O. G., (2004). "Radial superlattices and single nanoreactors", *Appl. Phys. Lett.*, 84: 4475-4477.
12. Prinz, A. V., Prinz, V. Ya., Seleznev, V. A., (2003). "Semiconductor Micro- and Nanoneedles for Microinjections and Ink-Jet Printing", *Microelectron. Eng.*, 67/68: 782-788.
13. Eringen, A. C., (1983). "On Differential Equations of Nonlocal Elasticity and Solutions of Screw Dislocation and Surface Waves", *J. Appl. Phys.*, 54: 4703-4710.
14. Eringen, A. C., (2002). "*Nonlocal Continuum Field Theories*", Springer, New York.

15. Yan, J. W., Tong, L. H., Li, C., Zhu, Y., Wang, Z. W., (2015). "Exact solutions of bending deflections for nano-beams and nano-plates based on nonlocal elasticity theory", *Compos. Struct.*, 125: 304–313.
16. Dastjerdi, S., Jabbarzadeh, M., (2016). "Nonlinear bending analysis of bilayer orthotropic graphene sheets resting on Winkler–Pasternak elastic foundation based on non-local continuum mechanics", *Compos. Part B: Eng.*, 87: 161–175.
17. Ansari, R., Faghieh Shojaei, M., Shahabodini, A., Bazdid-Vahdati, M., (2015). "Three-dimensional bending and vibration analysis of functionally graded nanoplates by a novel differential quadrature-based approach", *Compos. Struct.*, 131: 753–764.
18. Rahmani, O., Asemani, S.S., Hosseini, S. A., (2016). "Study the Surface Effect on the Buckling of Nanowires Embedded in Winkler–Pasternak Elastic Medium Based on a Nonlocal Theory", *J. Nanostruct.*, 6: 87-92.
19. Ansari, R., Rouhi, H., (2012). "Nonlocal Flugge shell model for thermal buckling of multi-walled carbon nanotubes with layerwise boundary conditions", *J. Therm. Stresses*, 35: 326-341.
20. Rouhi, H., Ansari, R., (2012). "Nonlocal analytical Flugge shell model for axial buckling of double-walled carbon nanotubes with different end conditions", *NANO*, 7: 1250018.
21. Zamani Nejad, M., Hadi, A., Rastgoo, A., (2016). "Buckling analysis of arbitrary two-directional functionally graded Euler–Bernoulli nano-beams based on nonlocal elasticity theory", *Int. J. Eng. Sci.*, 103: 1–10.
22. Ansari, R., Rouhi, H., (2015). "Nonlocal Flügge shell model for the axial buckling of single-walled carbon nanotubes: An analytical approach", *Int. J. Nano Dimen.*, 6: 453-462.
23. Ghorbanpour-Arani, A., Shokravi, M., (2013). "Nonlocal Vibration Behavior of a Viscoelastic SLGS Embedded on Visco-Pasternak Foundation Under Magnetic Field", *J. Nanostruct.*, 3: 467- 476.
24. Ansari, R., Arash, B., Rouhi, H., (2011). "Vibration characteristics of embedded multi-layered graphene sheets with different boundary conditions via nonlocal elasticity", *Compos. Struct.*, 93: 2419–2429.
25. Ansari, R., Rouhi, H., Arash, B., (2013). "Vibrational analysis of double-walled carbon nanotubes based on the nonlocal Donnell shell theory via a new numerical approach", *Iranian J. Sci. Technol. Trans. Mech. Eng.*, 37: 91-105.
26. Farajpour, A., Hairi Yazdi, M. R., Rastgoo, A., Loghmani, M., Mohammadi, M., (2016). "Nonlocal nonlinear plate model for large amplitude vibration of magneto-electro-elastic nanoplates", *Compos. Struct.*, 140: 323–336.
27. Ansari, R., Gholami, R., Rouhi, H., (2015). "Size-Dependent Nonlinear Forced Vibration Analysis of Magneto-Electro-Thermo-Elastic Timoshenko Nanobeams Based upon the Nonlocal Elasticity Theory", *Compos. Struct.*, 126: 216–226.
28. Pradhan, S. C., Kumar A., (2010). "Vibration analysis of orthotropic graphene sheets embedded in Pasternak elastic medium using nonlocal elasticity theory and differential quadrature method", *Comput. Mater. Sci.*, 50: 239-245.
29. Gurses, M., Akgoz, B., Civalek, O., (2012). "Mathematical modeling of vibration problem of nano-sized annular sector plates using the nonlocal continuum theory via eight-node discrete singular convolution transformation", *Appl. Math. Comput.*, 219: 3226–3240.
30. Ansari, R., Rouhi, H., Sahmani, S., (2011). "Calibration of the Analytical Nonlocal Shell Model for Vibrations of Double-Walled Carbon Nanotubes with Arbitrary Boundary Conditions Using Molecular Dynamics", *Int. J. Mech. Sci.*, 53: 786-792.
31. Ansari, R., Rouhi, H., (2012). "Analytical Treatment of the Free Vibration of Single-Walled Carbon Nanotubes Based on the Nonlocal Flugge Shell Theory", *J. Eng. Mater. Technol.*, 134: 011008.
32. Ansari, R., Rouhi, H., (2012). "Explicit Analytical Expressions for the Critical Buckling Stresses in a Monolayer Graphene Sheet Based on Nonlocal Elasticity", *Solid State Commun.*, 152: 56-59.
33. Shen, H. S., Xu, Y. M., Zhang, C. L., (2013). "Prediction of Nonlinear Vibration of Bilayer Graphene Sheets in Thermal Environments via Molecular Dynamics Simulations and Nonlocal Elasticity", *Comput. Meth. Appl. Mech. Eng.*, 267: 458–470.
34. Liang, Y., Han, Q., (2014). "Prediction of the Nonlocal Scaling Parameter for Graphene Sheet", *Eur. J. Mech. - A/Solids*, 45: 153–160.
35. Nazemnezhad, R., Hosseini-Hashemi, S., (2014). "Free Vibration Analysis of Multi-Layer Graphene Nanoribbons Incorporating Interlayer Shear Effect via Molecular Dynamics Simulations and Nonlocal Elasticity", *Phys. Lett. A*, 378: 3225–3232.
36. Gurtin, M. E., Murdoch, A. I., (1975). "A Continuum Theory of Elastic Material Surfaces", *Arch. Rat. Mech. Anal.*, 57: 291-323.
37. Gurtin, M. E., Murdoch, A. I., (1978). "Surface Stress in Solids", *Int. J. Solids Struct.*, 14: 431-440.
38. Gibbs, J. W., (1906). "*The Scientific Papers of J. Willard Gibbs*", Vol. 1., Longmans-Green, London.
39. Ghorbanpour-Arani, A., Zarei, M. Sh., (2015). "Surface Effect on Vibration of Y-SWCNTs Embedded on Pasternak Foundation Conveying Viscose Fluid", *J. Nanostruct.*, 5; 33-40.

40. Ansari, R., Mohammadi, V., Faghieh Shojaei, M., Gholami, R., Sahmani, S., (2013). "Postbuckling characteristics of nanobeams based on the surface elasticity theory", *Compos. Part B: Eng.*, 55: 240–246.
41. Assadi, A., Farshi, B., (2011). "Size Dependent Vibration of Curved Nanobeams and Rings Including Surface Energies", *Physica E*, 43: 975-978.
42. Ansari, R., Mohammadi, V., Faghieh Shojaei, M., Gholami, R., Rouhi, H., (2014). "Nonlinear Vibration Analysis of Timoshenko Nanobeams Based on Surface Stress Elasticity Theory", *Eur. J. Mech. A/Solids*, 45: 143-152.
43. Dai, H. L., Zhao, D. M., Zou, J. J., Wang, L., (2016). "Surface effect on the nonlinear forced vibration of cantilevered nanobeams", *Physica E*, 80: 25-30.
44. Ansari, R., Mohammadi, V., Faghieh Shojaei, M., Gholami, R., Sahmani, S., (2014). "On the forced vibration analysis of Timoshenko nanobeams based on the surface stress elasticity theory", *Compos. Part B: Eng.*, 60: 158–166.
45. Song, F., Huang, G. L., (2009). "Modeling of Surface Stress Effects on Bending Behavior of Nanowires: Incremental Deformation Theory", *Phys. Lett. A*, 373: 3969-3973.
46. Chiu, M. S., Chen, T., (2013). "Bending and Resonance Behavior of Nanowires Based on Timoshenko Beam Theory with High-Order Surface Stress Effects", *Physica E*, 54: 149-156.
47. Kiani, K., (2015). "Stability and vibrations of doubly parallel current-carrying nanowires immersed in a longitudinal magnetic field", *Phys. Lett. A*, 379: 348–360.
48. Narendar, S., Gopalakrishnan, S., (2012). "Study of Terahertz Wave Propagation Properties in Nanoplates with Surface and Small-Scale Effects", *Int. J. Mech. Sci.*, 64: 221-231.
49. Ansari, R., Sahmani, S., (2011). "Surface stress effects on the free vibration behavior of nanoplates", *Int. J. Eng. Sci.*, 49: 1204–1215.
50. Assadi, A., (2013). "Size Dependent Forced Vibration of Nanoplates with Consideration of Surface Effects", *App. Math. Model.*, 37: 3575-3588.
51. Ansari, R., Gholami, R., Faghieh Shojaei, M., Mohammadi, V., Darabi, M. A., (2012). "Surface stress effect on the pull-in instability of hydrostatically and electrostatically actuated rectangular nanoplates with various edge supports", *J. Eng. Mater. Technol.*, 134: 041013.
52. Ansari, R., Mohammadi, V., Faghieh Shojaei, M., Gholami, R., Darabi, M. A., (2014). "A geometrically non-linear plate model including surface stress effect for the pull-in instability analysis of rectangular nanoplates under hydrostatic and electrostatic actuations", *Int. J. Non-Linear Mech.*, 67: 16–26.
53. Ansari, R., Gholami, R., (2016). "Size-dependent modeling of the free vibration characteristics of postbuckled third-order shear deformable rectangular nanoplates based on the surface stress elasticity theory", *Compos. Part B*, 95: 301-316.
54. Zhou, Y., (2015). "The surface effect on axisymmetric wave propagation in piezoelectric cylindrical shells", *Adv. Mech. Eng.*, DOI: 10.1177/1687814014568503.
55. Rouhi, H., Ansari, R., Darvizeh, M., (2016). "Size-dependent free vibration analysis of nanoshells based on the surface stress elasticity", *Appl. Math. Model.*, 40: 3128–3140.
56. Flugge, W., (1960). "Stresses in Shells", Springer, Berlin.
57. Reddy, J. N., (2004). "Mechanics of laminated composite plates and shells", 2nd ed., CRC Press, New York.
58. Lu, P., He, L. H., Lee, H. P., Lu, C., (2006). "Thin plate theory including surface effects", *Int. J. Solids Struct.*, 43: 4631–4647.
59. Nayfeh, A. H., (1993). "Introduction to Perturbation Techniques", Wiley, New York.
60. Miller, R. E., Shenoy, V. B., (2000). "Size-Dependent Elastic Properties of Nanosized Structural Elements", *Nanotechnology*, 11: 139-147.
61. Zhu, R., Pan, E., Chung, P. W., Cai, X., Liew, K. M., Buldum, A., (2006). "Atomistic Calculation of Elastic Moduli in Strained Silicon", *Semicond. Sci. Technol.*, 21: 906-911.
62. Ansari, R., Gholami, R., Norouzzadeh, A., Darabi, M. A., (2015). "Surface Stress Effect on the Vibration and Instability of Nanoscale Pipes Conveying Fluid Based on a Size-Dependent Timoshenko Beam Model", *Acta Mechanica Sinica*, 31: 708-719.